Update: Cardiac Imaging (VIII)

Myocardial Mapping With Cardiac Magnetic Resonance: The Diagnostic Value of Novel Sequences

Javier Sanz,[a,b,*] Gina LaRocca,[a] and Jesús G. Mirelis[b,c]

[a] *The Zena and Michael A. Wiener Cardiovascular Institute and Marie-Josee and Henry R. Kravis Center for Cardiovascular Health, Mount Sinai School of Medicine, New York, United States*
[b] *Centro Nacional de Investigaciones Cardiovasculares (CNIC), Madrid, Spain*
[c] *Servicio de Cardiología, Hospital Universitario Puerta de Hierro, Majadahonda, Madrid, Spain*

A B S T R A C T

Cardiac magnetic resonance has evolved into a crucial modality for the evaluation of cardiomyopathy due to its ability to characterize myocardial structure and function. In the last few years, interest has increased in the potential of "mapping" techniques that provide direct and objective quantification of myocardial properties such as T_1, T_2, and T_2^* times. These approaches enable the detection of abnormalities that affect the myocardium in a diffuse fashion and/or may be too subtle for visual recognition. This article reviews the current state of myocardial T_1 and T_2-mapping in both health and disease.

© 2016 Sociedad Española de Cardiología. Published by Elsevier España, S.L.U. All rights reserved.

Mapeo miocárdico con resonancia magnética cardiaca: valor diagnóstico de las nuevas secuencias

R E S U M E N

La resonancia magnética cardiaca ha evolucionado hasta convertirse en una modalidad diagnóstica esencial en la evaluación de la miocardiopatía, gracias a su capacidad para caracterizar la estructura y la función del miocardio. En los últimos años ha aumentado el interés en el potencial de las técnicas de mapeo que aportan una cuantificación directa y objetiva de las propiedades del miocardio, como los tiempos T_1, T_2 y T_2^*. Estos métodos permiten detectar anomalías que afectan al miocardio de manera difusa o son demasiado sutiles para identificarlas en un examen visual. En este artículo se revisa el estado actual del mapeo miocárdico T_1 y T_2 tanto en salud como en enfermedad.

© 2016 Sociedad Española de Cardiología. Publicado por Elsevier España, S.L.U. Todos los derechos reservados.

INTRODUCTION

Standard approaches for myocardial characterization with cardiac magnetic resonance (CMR) include T_1-weighted, T_2-weighted, and late gadolinium enhancement (LGE) imaging that allow the visualization of fatty infiltration, edema, or necrosis/scarring.[1] These sequences rely on relative changes in signal intensity between abnormal and normal myocardium. However, they are hampered by their often semiquantitative nature and their inherent limitations in depicting diffuse myocardial processes with no "normal" reference myocardium at the time of imaging. Myocardial mapping with CMR is quickly evolving as an objective and quantitative approach for the noninvasive characterization of myocardial properties such as extracellular volume expansion, edema, or other abnormalities in tissue composition. In this article, we review state-of-the-art myocardial T_1- and T_2- mapping in health and disease. Older T_2^*-mapping approaches that can detect iron overload or intramyocardial hemorrhage are reviewed elsewhere.[2]

T_1- AND T_2-MAPPING

A detailed description of the physics principles of CMR is beyond the scope of this review. Briefly, CMR generates images by transferring energy to ^1H water and fat protons, which is in turn released as they recover their baseline state ("relax"), and which can be detected and mapped into a spatial distribution of protons. The speed of this relaxation is determined by T_1 and T_2 (longitudinal and transverse relaxation times, respectively). T_1 and T_2 times are intrinsic tissue properties that also depend on the magnetic field strength: T_1 lengthens at higher fields whereas T_2 remains relatively constant,[3] although myocardial T_2 tends to shorten.[4] Gadolinium-based contrast agents change relaxation times, specifically shortening T_1.

A T_1- or T_2-map is an image in which signal intensity in each voxel is directly proportional to the T_1 or T_2 time of the tissue within. These times can be compared with those of remote

* Corresponding author: Cardiovascular Institute, Mount Sinai Hospital, One Gustave L Levy Place, Box 1030, New York, NY 10029, United States.
E-mail address: Javier.Sanz@mssm.edu (J. Sanz).

myocardium in focal or heterogeneous processes, or with normal reference values in cases of diffuse disease. While LGE detects localized replacement fibrosis,[5] T_1-mapping techniques were initially developed to study diffuse interstitial fibrosis, although their applications continue to expand. The main purpose of T_2-mapping is the detection of edema.[2]

Native T_1 Time

One potential application of T_1-mapping is the quantification of native (or precontrast) myocardial T_1 (Figure 1A). Native T_1 can be prolonged or shortened in a variety of clinical conditions (see below). Since contrast administration is not needed, native T_1-mapping offers diagnostic potential in patients with relative contraindications to gadolinium (ie, advanced renal failure). The histopathological correlates of T_1 remain incompletely elucidated, but T_1 reflects changes in both the intracellular and extracellular compartments, and is influenced by the presence of edema, collagen or other proteins, iron, and lipids.[6]

Postcontrast T_1 Time

T_1 can be calculated after the administration of gadolinium (Figure 1B). Most gadolinium agents are extracellular compounds: they distribute in the intravascular and interstitial compartments but not within the cells. Thus, reduced postcontrast T_1 either reflects access to the intracellular space (loss of cell membrane integrity in, for example, acute necrosis) and/or interstitial space expansion that is largely considered a surrogate of interstitial fibrosis.[7] Although this was the first approach for clinical myocardial T_1-mapping,[8] postcontrast T_1 use has fallen somewhat out of favor because of its dependency on time after gadolinium administration, contrast dose, body composition, renal clearance, heart rate, and hematocrit.[5] Approaches to correct for these variations have nonetheless been proposed.[9–12]

Partition Coefficient (λ)

λ represents the relationship between changes in pre- and postcontrast myocardium and blood T_1 and is calculated as:
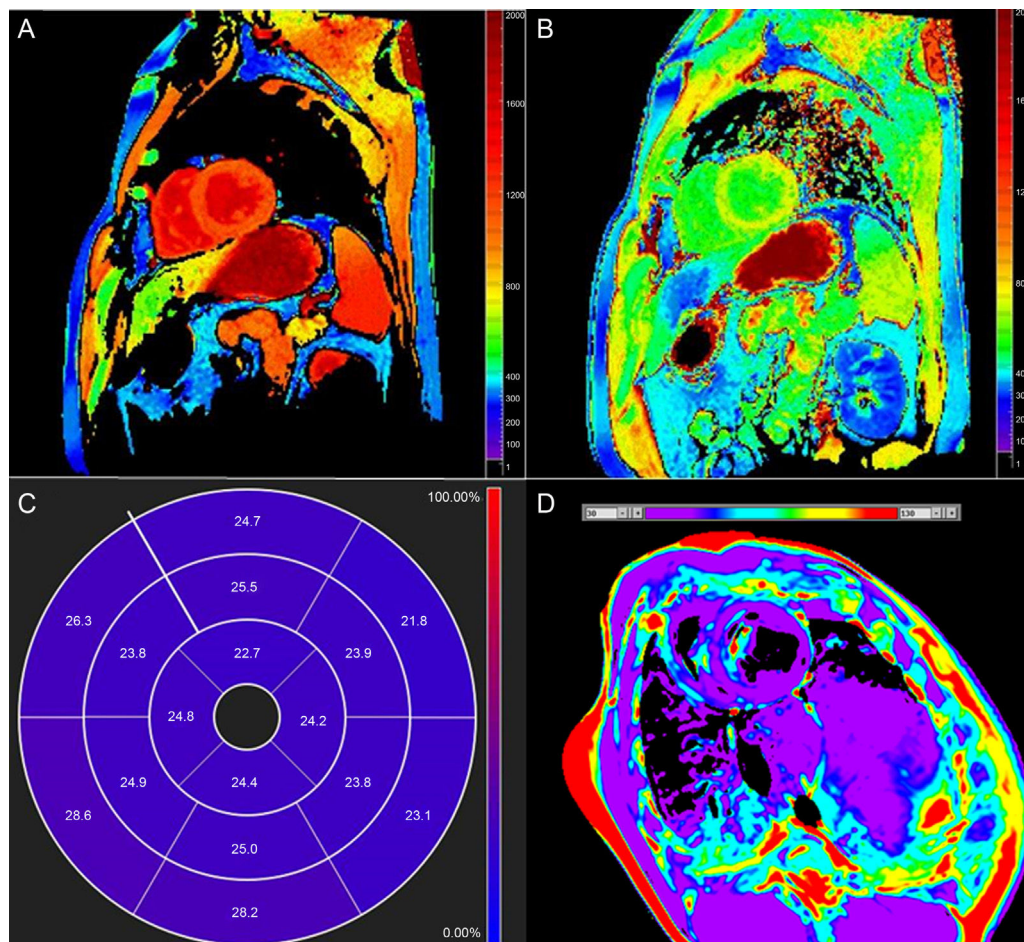
$$\lambda = \Delta R1_{myoc} / \Delta R1_{blood}$$

Figure 1. Native myocardial T_1 map (A), postcontrast T_1 map (B), 17-segment extracellular volume diagram (C) and T2 map (D). A-C: normal individual; D: normal experimental animal.

where *R1* is tissue relaxivity (1/T1) and *ΔR1* is $R1_{postcontrast}$ − $R1_{precontrast}$[13]

λ attempts to account for interindividual variations in contrast dose, time after contrast or renal clearance by correcting for precontrast T_1 as well blood T_1 changes, and is also less sensitive to magnetic field strength.[14] However, it remains sensitive to some confounders, particularly blood plasma volume (see below).

Extracellular Volume

Extracellular volume (ECV) (Figure 1C) incorporates a correction for blood plasma volume and is calculated as:[13]

$$ECV = \lambda \cdot (1 - hematocrit)$$

ECV maps can also be generated. Ideally, hematocrit should be quantified simultaneously to the CMR scan;[6,15] however, this recommendation has been challenged based on logistical considerations as well as considerable variability in hematocrit determinations.[16] Furthermore, an approach using hematocrit estimated from blood R1 has recently been proposed and validated[16] that may obviate the need for actual quantification.

In normal conditions, the extracellular space represents approximately 25% of myocardial volume.[5,15] Extracellular volume combines both the interstitial and intravascular space and, similar to postcontrast T_1, is often considered a surrogate of interstitial fibrosis.[15] Extracellular volume can be quantified during a slow, continuous infusion of contrast or reasonably approximated at least 15 min after a bolus injection,[17,18] although the latter tends to overestimate large ECV values.[18] While ECV is less sensitive to confounding factors, the sequences used may still be prone to errors and some influence of gadolinium concentration (in turn influenced by contrast dose, postcontrast delay, or body habitus) remains.[6,17,19,20]

Today, native T_1 and ECV are the preferred indices derived from T_1-mapping.[6]

Native T_2 Time

T_2 time lengthens in proportion to water content,[21] and consequently increased T_2 largely reflects myocardial edema. Standard T_2-weighted images are limited because of susceptibility to artifacts and subjective interpretation, so T_2-mapping (Figure 1D) offers the potential for more objective detection and quantification of inflammation and/or reperfusion related edema.

T_1 AND T_2 QUANTIFICATION

Cardiac magnetic resonance sequences for T_1-mapping rely on the generation of images at different degrees of longitudinal relaxation to generate a signal intensity vs time curve (Figure 2) from which T_1 is calculated. This can be accomplished by repeated acquisitions with varying inversion-recovery times[8,22]; however, this requires multiple breath-holds. Thus, sequences have been designed that enable acquisition of all necessary images in a single breath-hold and in the same phase of the cardiac cycle. The first one, developed in 2004, is termed modified look-locker inversion recovery (MOLLI).[23] A number of modifications of MOLLI and alternative approaches have been proposed,[15,24] including a shortened version (shMOLLI) that allows for reduced breath-holding.[12]

Similarly, T_2-mapping relies on fitting a curve of signal intensity values on different times during transverse relaxation (Figure 3). This is typically achieved by using preparatory T_2 pulses[25] or different echo times during acquisition,[26] with different sequences showing specific strengths and limitations.[4] Although less pronounced and systematically explored in comparison with T_1-mapping, some potential heart rate dependency of measured T_2 values has been described.[27,28]

Normal T_1 and T_2 Values

Normal values for native myocardial T_1 times and ECV[19,28–39] are shown in Table 1. Native T_1 time at 1.5 T is approximately 900-1000 ms (longer at 3 T), whereas normal ECV is in the order of 20% to 30%, in good agreement with expected values.[5] As noted before, postcontrast T_1 times depend on several technical and physiological factors, and reported normal λ values have ranged from 0.25 to 0.70.[19,29,36] Multiple publications have reported increasing ECV with age.[19,28,35,38,40] The largest study to date with 1231 individuals[36] confirmed these associations, particularly in men, and reported higher precontrast T_1 and ECV in women, as also noted by others.[34,41] The presence of abnormal T_1-based indices, particularly native T_1 and ECV, allows for the identification of diseased
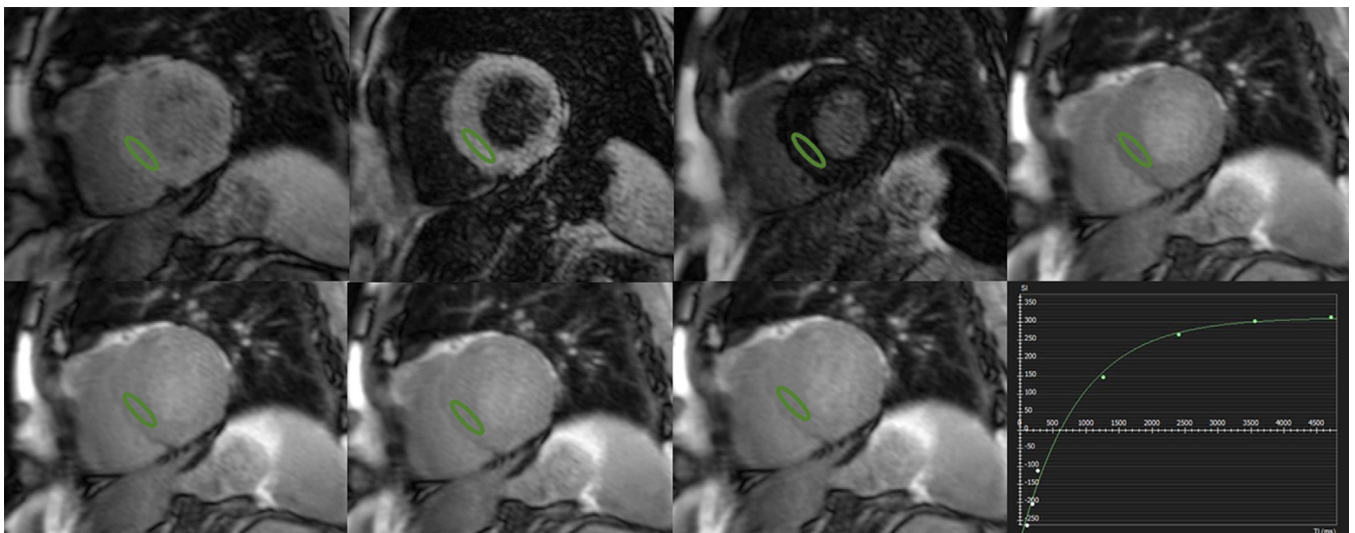

Figure 2. Images with increasing inversion times are acquired (left to right and top to bottom), and signal intensity (in this case in the septum) is plotted against inversion times to obtain the T_1 time.
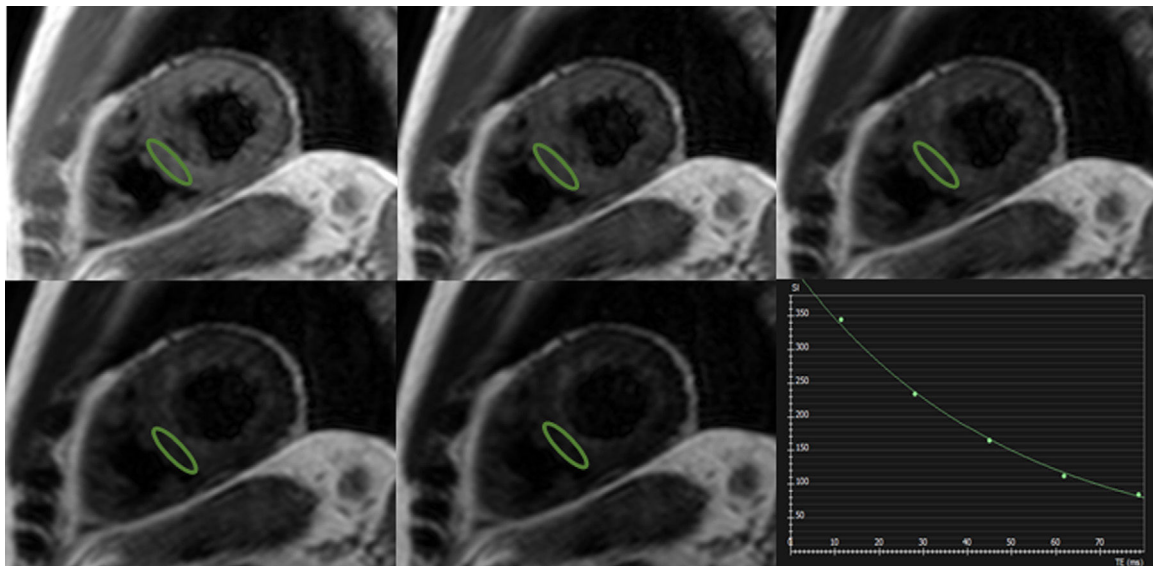
Figure 3. Images with increasing echo times are acquired (left to right and top to bottom), and signal intensity (in this case in the septum) is plotted against echo times to obtain the T_2 time.

myocardium,[29,33,34,40] and respective thresholds of approximately 1000 ms (at 1.5 T) and 30% have been used.[33,42–45] In 52 patients with either dilated or hypertrophic cardiomyopathy (DCM and HCM, respectively) and 30 controls, native T_1 showed the highest accuracy in differentiating between healthy and diseased myocardium with a sensitivity of 100%, specificity of 96%, and diagnostic accuracy of 98% (area under the curve = 0.99; 95% confidence interval [95%CI], 0.96-1.00; $P < .001$).[37]

Table 2 summarizes normal myocardial T_2 values.[4,27,28,32,46–48] At 1.5 T, T_2 is in the order of 50-60 ms (slightly shorter at 3 T) and a possible increase with aging has been reported.[49] Although far less

validated, T_2 can also be used to differentiate normal from abnormal myocardium with a cutoff in the vicinity of 60 ms.[27,50–52]

VALIDATION OF T_1- AND T_2-MAPPING

Beyond phantom and animal experiments, T_1-mapping techniques have been validated against histology of human myocardium[8,16,18,22,31,41,43,53–60] (Table 3). Importantly, these studies comprise a variety of clinical scenarios including HCM, DCM, heart failure with preserved ejection fraction, end-stage heart failure, or valvular heart disease. Most studies used endomyocardial biopsy

Table 1

Normal Myocardial Native T_1 Times and Extracellular Volume (Studies With $\geq$ 30 Participants)

Study	No.	Sequence	Native T_1, ms	ECV, %
1.5 T				
Dabir et al.[19]	34	MOLLI	950 ± 21	25 ± 4
Rogers et al.[29]	38	MOLLI	952 ± 41	NA
Reiter et al.[30]	40	MOLLI[a]	984 ± 28	NA
Fontana et al.[31]	50	shMOLLI	NA	27 ± 3
		IR-GRE	NA	26 ± 3
Luetkens et al.[32]	50	MOLLI	967 ± 28	27.7 ± 5.8
		shMOLLI	831 ± 27	25 ± 4.5
Kellman et al.[33]	62	MOLLI[a]	965 ± 35	25.4 ± 2.5
Sado et al.[34]	81	IR-GRE	NA	25.3 ± 2.9
Piechnik et al.[35]	342	shMOLLI	953 ± 23	NA
Liu et al.[36]	625 women	MOLLI	986 ± 45	28.1 ± 2.8
	606 men		968 ± 38	25.8 ± 2.9
3 T				
Puntmann et al.[37]	30	MOLLI	1070 ± 55	27 ± 9
Neilan et al.[38]	32	Look-locker	NA	28 ± 3
Dabir et al.[19]	32	MOLLI	1052 ± 23	26 ± 4
Rogers et al.[29]	38	MOLLI	1087 ± 60	NA
Von Knobelsdorff-Brenkenhoff et al.[28]	60	MOLLI	1158.8 (1074.0-1250.1)[b]	NA
Liu et al.[39,c]	92	MOLLI	1232 ± 51	NA

ECV, extracellular volume; IR-GRE, inversion-recovery gradient recalled echo; MOLLI, modified look-locker inversion recovery, NA, not applicable; shMOLLI, short MOLLI.
T_1 times and extracellular volume values expressed as mean ± standard deviation.
  [a] Modified MOLLI.
  [b] Mean (95% confidence intervals).
  [c] African Americans.

Table 2

Normal Myocardial Native Myocardial T_2 Times (Studies With ≥ 20 Participants)

Study	No	Sequence	Native T_2, ms
1.5 T			
Sprinkart et al.[26]	20	GraSE	52.2 ± 2
Radunski et al.[46]	21	T2-SSFP	55 [54-60][a]
Mordi et al.[47]	21	T2-SSFP	52.9 ± 3.3
Thavendiranathan et al.[27]	30	T2-SSFP	54.5 ± 2.2
Baessler et al.[4]	30	GraSE	58.6 ± 4.2
		T2-SSFP	52.5 ± 2.5
Luetkens et al.[32]	50	GraSE	52.4 ± 2.6
Wassmuth et al.[48]	69	T2-SSFP	55 ± 5
		T2-GRE	52 ± 5
3 T			
Baessler et al.[4]	30	GraSE	54.2 ± 4.1
		T2-SSFP	44 ± 3.2
Von Knobelsdorff-Brenkenhoff et al.[28,a]	60	T2-SSFP	45.1 (39.9-50.1)[b]

GraSE, gradient-spin-echo sequence; T_2-GRE, T_2-prepared gradient recalled echo; T_2-SSFP, T_2-prepared steady state free precession.
T_2 times expressed as mean ± standard deviation.
^a Median [interquartile range].
[a] Median [interquartile range].
[b] Mean (95% confidence intervals).

for validation, although 2 evaluated whole explanted hearts. Two reports demonstrated significant correlations of native T_1 with collagen volume fraction, although a third study failed to find a significant association. Most studies also identified significant correlations between postcontrast T_1 and collagen amount, typically less consistent than for ECV (Table 3). Extracellular volume tends to provide higher values than collagen volume fraction, probably reflecting the fact that the interstitial space is not occupied by connective tissue exclusively.

Histological validation of T_2-mapping is much scantier. So far, only 1 investigation has demonstrated T_2 elevation in biopsy-proven myocarditis,[51] and 1 modern T_2-mapping sequence has been compared with actual myocardial water content at contemporary field strengths.[61]

CLINICAL T_1- AND T_2-MAPPING

T_1-mapping has been most extensively employed in clinical studies. With the exception of iron and lipid accumulation, myocardial diseases lead to elevations in native T_1 (Table 4). Not surprisingly, ECV also increases in most disorders, particularly in myocardial infarction (MI) and amyloidosis (Table 4). T_2-mapping has been mostly used in acute ischemic and inflammatory disease.

Clinical and Preclinical Heart Failure

Reduced postcontrast T_1 time has been demonstrated in both heart failure with reduced left ventricular (LV) ejection fraction and heart failure with preserved ejection fraction, with correlations with the degree of diastolic dysfunction.[8,57] An increase in native T_1 and ECV has also been reported and validated in DCM.[37,43] Myocardial mapping of T2, ECV and, particularly, native

Table 3

Validation Studies of T_1-mapping Against Histopathology (Collagen Volume Fraction)

Study	Population	No.	Sequence	Field strength (T)	Correlation with CVF (r)
Native T_1					
Bull et al.[53]	AS	19	shMOLLI	1.5	0.65
Lee et al.[54]	AS	20	MOLLI	3	0.77
De Meester de Ravenstein et al.[55]	VHD	31	MOLLI	3	−0.18[a]
Postcontrast T1					
Iles et al.[8]	Transplant	6	GRE-VAST	1.5	−0.70
Sibley et al.[56]	Various	47	Look-locker	1.5	−0.57
Mascherbauer et al.[57]	HFpEF	9	IR-GRE	1.5	−0.98
White et al.[18]	AS	18	shMOLLI	1.5	−0.46
Iles et al.[58]	ESHF[b]/HCM	12	GRE-VAST	1.5	−0.64
Miller et al.[41]	ESHF[b]	6	MOLLI	1.5	−0.74
Ellims et al.[59]	HCM	9	GRE-VAST	1.5	−0.70
De Meester de Ravenstein et al.[55]	VHD	31	MOLLI	3	−0.36[a]
ECV					
Flet et al.[22]	AS/HCM	26	IR-GRE	1.5	0.89
Fontana et al.[31]	AS	18	shMOLLI	1.5	0.83
Mille et al.[41]	ESHF[b]	6	MOLLI	1.5	0.75
White et al.[18]	AS	18	shMOLLI	1.5	0.83
aus dem Siepen et al.[43]	DCM	24	MOLLI	1.5	0.85
Kammerlander et al.[60]	Various	36	MOLLI[c]	1.5	0.49
Treibel et al.[16,d]	AS	18	shMOLLI	1.5	0.78
De Meester de Ravenstein et al.[55]	VHD	31	MOLLI	3	0.78

AS, aortic stenosis; CVF, collagen volume fraction; DCM, dilated cardiomyopathy; ECV, extracellular volume; ESHF, end-stage heart failure; GRE, gradient recalled echo; HCM, hypertrophic cardiomyopathy; HFpEF, heart failure with preserved ejection fraction; IR, inversion recovery; MOLLI, modified look-locker Inversion recovery; r, correlation coefficient; shMOLLI, short MOLLI; VAST, variable temporal sampling of k-space; VHD, valvular heart disease.
[a] Nonsignificant.
[b] Whole heart.
[c] Modified MOLLI.
[d] Estimated hematocrit.

Table 4

Changes in Native T_1 and Extracellular Volume in Different Diseases

	Native T_1	Extracellular volume
Hypertension	↑	↑
Diabetes mellitus	↑	↑
Heart failure with preserved ejection fraction	↑	↑
Acute myocardial infarction	↑↑	↑↑
Chronic myocardial infarction	↑	↑↑
Myocarditis	↑↑	↑
Other inflammatory cardiomyopathies	↑	↑
Amyloidosis	↑↑	↑↑
Anderson-Fabry disease	↓	↔
Hemosiderosis	↓	↔ ↑
Hypertrophic cardiomyopathy	↑	↑
Dilated cardiomyopathy	↑	↑
Congenital heart disease	?	↑
Valvular disease	↑	↑

↑: increase; ↓: decrease; ↔: unchanged; ?: unknown.

T_1 was found useful in the identification of early stages of nonischemic DCM and its differentiation from athlete's heart in a recent study.[47]

Cardiovascular risk factors that contribute to heart failure, particularly heart failure with preserved ejection fraction, include but are not limited to arterial hypertension and diabetes mellitus. Recent studies demonstrated increased native T_1 and ECV in the presence of hypertensive heart disease, defined as LV hypertrophy and/or altered mechanics, but not hypertension alone.[62] An independent increase of ECV has also been shown in diabetes.[63] Furthermore, abnormal T_1-mapping indices suggestive of fibrosis are associated with increasing cardiovascular risk scores in the general population, particularly in men.[64] Both in apparently healthy individuals and in disease, T_1 indices have been linked to LV systolic and diastolic dysfunction, remodeling, and impaired energetics, even in the absence of LGE.[20,40,42,65,66]

In pulmonary hypertension, an increase in ECV has been demonstrated in the right ventricular insertion points at the septum in a large animal model[67] and more recently in the free wall in patients,[68] with a significant association with pulmonary hemodynamics and right ventricular performance.

Ischemic Heart Disease

Cardiac magnetic resonance imaging is highly accurate for determining ventricular volumes and ventricular function and has the additional advantage of being able to characterize the myocardium and demonstrate changes associated with the ischemic insult such as necrosis/fibrosis, edema, microvascular obstruction, and intramyocardial hemorrhage.[69] Native T_1- and T_2-mapping can be used to detect myocardial edema in acute ischemic injury with higher accuracy and reproducibility than standard T_2-weighted imaging.[70,71] Sizing of the area-at-risk based on T_1 and/or T_2 elevations has been validated against fluorescent microspheres in animal models[72] and scintigraphy in patients.[44] T_2-mapping has also enabled quantitative analysis of edema temporal evolution after MI.[73]

In the setting of MI, T_1-mapping was used in an early study to evaluate acute (8 days) and chronic (6 months) infarct. Elevated native T_1 (3 standard deviations above remote myocardium)

detected acute MI with sensitivity and specificity of 96% and 91%, respectively, whereas postcontrast T1 was superior for the identification of chronic MI.[74] Not surprisingly, ECV in infarcted regions is markedly elevated, typically $\geq$ 50%.[33,34,75] Native T_1 times are highest in the acute stage and tend to overestimate infarct size, consistent with higher edema content,[74,75] and while they subsequently remain elevated, specificity is high but sensitivity is modest for the detection of chronic MI.[76] T_2 times are also elevated with acute MI (Figure 4), in which T_2-mapping is again superior to standard T_2-weighted imaging.[50] T_1 and T_2 are reduced in the presence of microvascular obstruction and/or intramyocardial hemorrhage,[50,75] and decreased native T_1 in the MI core has been linked to an increased risk of subsequent death or hospitalization for heart failure.[77]

The feasibility of detecting ischemia during pharmacologic stress without contrast agents measuring changes in myocardial native T_1 has been reported recently.[78]

Inflammatory Cardiomyopathies

Myocarditis

The standard approach for the diagnosis of acute myocarditis on CMR relies on the combination of different techniques including T_2-weighted imaging, early gadolinium enhancement, and LGE (Lake-Louise criteria).[79] However, growing data demonstrate the superior diagnostic performance of myocardial mapping. T_2 is abnormally elevated in acute myocarditis even in the absence of LGE or visually apparent wall motion abnormalities, and outperforms standard T_2-weighted imaging.[27] In 50 patients with suspected acute myocarditis (median time from clinical presentation, 3 days), native T_1 time $\geq$ 990 ms had 90% sensitivity and 91% specificity and accuracy for the differentiation from controls. It had higher sensitivity than T_2-weighted imaging and LGE, which may be especially useful in detecting subtle focal disease and when gadolinium administration is not feasible.[45] In another publication by the same group, native T_1-mapping detected significantly larger areas of involvement than T_2-weighted and LGE imaging, identified areas of injury where these techniques were negative, and improved diagnostic confidence in an additional 30% of cases.[80] Similar findings of increased accuracy of native T_1 vs Lake-Louise criteria and even ECV were reported in suspected myocarditis (median, symptom duration, 3 days) using a threshold of native T_1 $\geq$ 1140 ms at 3 T.[81] In a more recent study, the same authors performed myocardial mapping in 34 patients with suspected acute myocarditis (median time also 3 days) as well as standard CMR and longitudinal strain quantification. Native T_1- and T_2-mapping demonstrated the highest accuracy (areas under the curve of 0.95 and 0.92, respectively), superior to ECV and standard criteria, which improved to 0.98 when native T_1 and LGE were combined.[32]

Another investigation evaluated 104 patients with clinically diagnosed acute/subacute myocarditis (median time from symptom onset, 2 weeks) and presenting with either heart failure or chest pain. Extracellular volume provided the single best diagnostic accuracy (76%) compared with native T_1- and T_2-mapping (69% and 63%, respectively), which were in turn similar to Lake-Louise criteria (accuracies of 59%-70%). A stepwise use of LGE (highly specific) followed by global myocardial ECV ($\geq$ 27%) if LGE was negative significantly improved the diagnostic accuracy in comparison with Lake-Louise criteria (90% vs 79%, P = .004).[46] A report of 165 patients with clinically diagnosed myocarditis divided the population into those with acute (n = 61, median time from presentation, 5 days) and convalescent stages (n = 67; median, 6 months). While native T_1-mapping
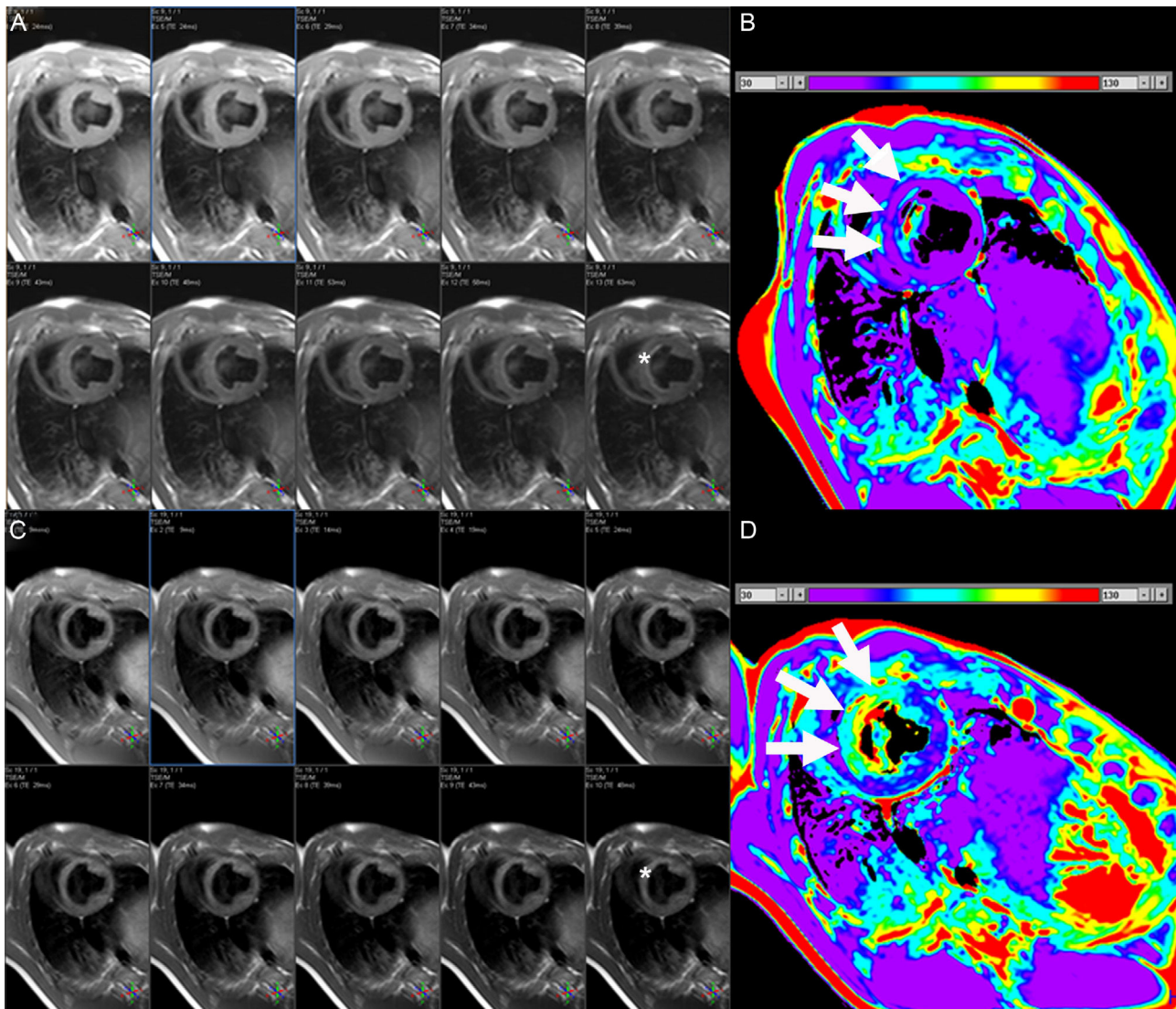
Figure 4. Consecutive short axis views of a T_2-mapping sequence with increasing echo times (A and C, from left to right and superior to inferior) and corresponding T_2 maps (B and D) in an animal at baseline (A and B), and after experimentally induced myocardial infarction (C and D). Note the different signal intensity with increasing echo times in the anteroseptum after the infarct but not at baseline (asterisks). The T_2 maps demonstrate normal T_2 values in the anteroseptum at baseline, but markedly increased after myocardial infarction (white arrows). The color bars indicate the color-coded range of T_2 values. Images courtesy of Dr. Javier Sánchez-González.

showed the highest accuracy (99%) in the acute phase, again outperforming standard CMR, in the convalescent phase, LGE was superior (accuracy 94%). The authors demonstrated that acute myocarditis can be independently identified by native T_1 > 5 standard deviations above the mean of the normal range, whereas convalescence was best defined by either abnormal native T_1 > 2 standard deviations and/or the presence of LGE, with subsequent validation in an independent cohort.[82]

In 31 patients with new-onset heart failure (median time from presentation, 1 month), T_2-mapping was able to distinguish between patients with and without histologically-proven inflammation with moderate accuracy (area under the curve = 0.78), whereas standard criteria, native T_1, and ECV were not.[51]

Altogether, these finding suggests a potentially important role of myocardial mapping in the evaluation of myocarditis although, and similar to Lake-Louise criteria, the accuracy and usefulness of different indices are likely dependent on clinical presentation and stage of the disease.

Other

Elevated native T_1 and T_2 times have been described in small series of patients with tako-tsubo cardiomyopathy.[27,71] Similarly, more than half of 50 patients with proven extracardiac sarcoid demonstrated elevated T_2 values regardless of the presence of LGE.[83] After heart transplant, myocardial T_2 lengthening can be a sign of ongoing or impending rejection, with normalization after immunosuppressive therapy.[52,84]

Preliminary studies indicate another potential use of CMR mapping for detecting cardiac involvement in autoimmune disorders. A series of 24 patients with systemic lupus erythematosus demonstrated increases in T_2 times compared with controls,

suggestive of subclinical myocardial inflammation.[85] Other studies have reported increases in native T_1 and ECV in rheumatoid arthritis and systemic scleroderma that correlate with markers of disease activity,[86,87] as well as in lupus,[88] independently of the presence of LGE. Whether these changes reflect inflammation, diffuse fibrosis, or both, is uncertain.

Infiltrative and Deposit Cardiomyopathies

Amyloidosis

In cardiac amyloidosis, CMR often demonstrates a characteristic pattern of global, predominantly subendocardial LGE coupled with abnormal myocardial and blood-pool gadolinium kinetics.[89] Although CMR is already highly accurate, T_1-mapping can provide additional information (Figure 5).

Native T_1 is abnormally increased in different forms of cardiac amyloidosis. In 51 patients with systemic light-chain amyloid, myocardial T_1 (1.5 T) was significantly elevated in those with cardiac involvement (1140 ± 61 ms) compared with normal participants (958 ± 20 ms; $P < .001$). T_1 was increased even when cardiac involvement was uncertain (1048 ± 48 ms) or thought absent (1009 ± 31 ms; $P < .01$ for both). A cutoff value of 1020 ms was 92% accurate for identifying possible or definite cardiac involvement.[90] Another series of 79 patients with light-chain and 85 with transthyretin amyloidosis demonstrated T_1 increases in both types that were significant in comparison with controls and HCM patients (area under the curve = 0.85 against the latter). T_1 time in transthyretin amyloidosis correlated with amyloid burden as determined by scintigraphy.[91] A larger study[92] confirmed these observations and the higher elevation of T_1 in light-chain (1126 ± 70 ms) compared with transthyretin amyloidosis (1101 ± 46 ms; $P < .05$). As mentioned earlier, ECV is markedly elevated in amyloidosis, typically in the range of 40% to 70%,[20,92–94] including segments without evident LGE or increased wall thickness.[93] Again there seem to exist differences between amyloid subtypes, with higher ECV in the transthyretin variant (58 ± 6% vs 54 ± 7%; $P = .001$).[92]

Extracellular volume and native myocardial T_1 correlate with markers of disease severity in amyloidosis, including wall thickness, systolic and diastolic dysfunction, electrocardiographic abnormalities, serum biomarkers, and functional class.[90,92–94]

Anderson-Fabry Disease

Anderson-Fabry disease is a rare but underdiagnosed intracellular lipid disorder with associated LV hypertrophy. As opposed to other infiltrative disorders, native T_1 is shortened but ECV remains normal, and the degree of reduction correlates with lipid content.[95] A study evaluated patients with Anderson-Fabry disease (n = 44) or LV hypertrophy of other etiologies (n = 105), and healthy controls (n = 67). Native septal T_1 was lower in Anderson-Fabry than in controls and was higher in hypertrophy (882 ± 47, 968 ± 32, and 1018 ± 74 ms, respectively; $P < .0001$). There was no overlap between Anderson-Fabry and other forms of hypertrophy and, importantly, it was abnormal in genetically positive patients with normal wall thickness.[96]
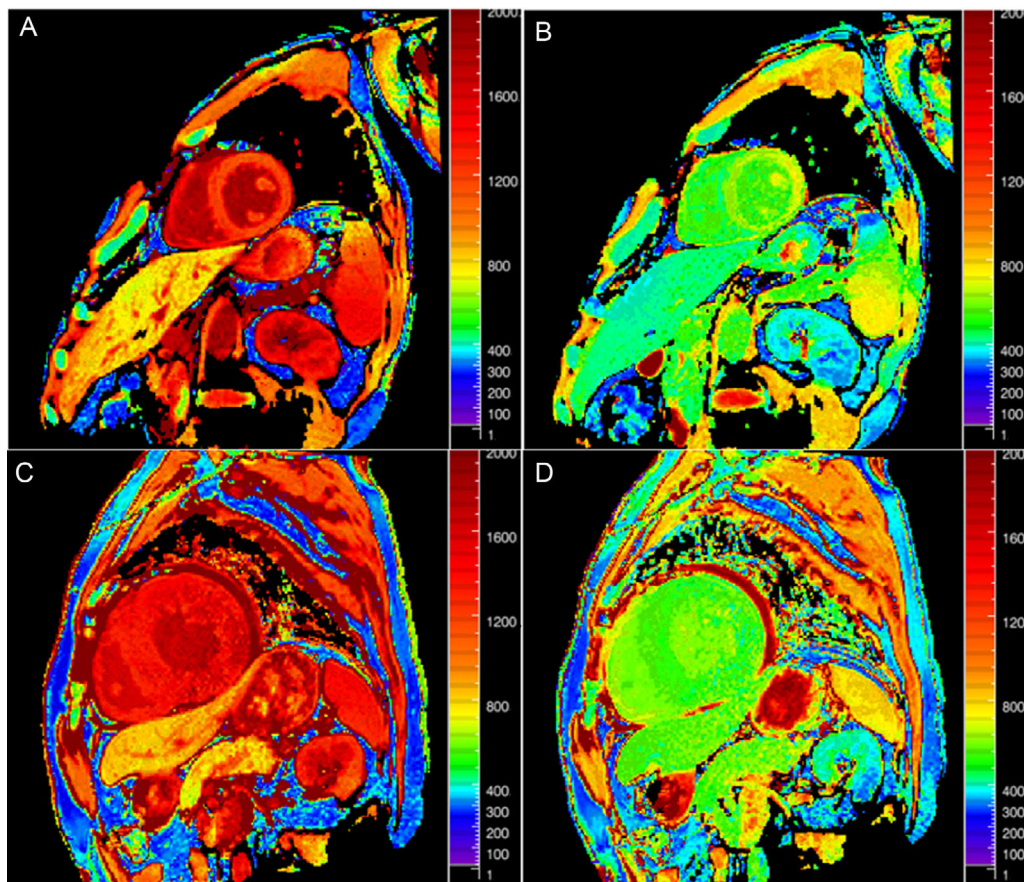

Figure 5. Native (A and C) and postcontrast (B and D) T_1 maps at 3 T in a patient without (upper row) and with cardiac amyloidosis (lower row). Note the increased native T_1 and decreased postcontrast T_1 in amyloidosis, translating into markedly increased extracellular volume (21% vs 46%, respectively).

Hemosiderosis

Iron overload is another condition causing significant T_1 shortening. Ferric iron alters the local magnetic field, usually characterized by the reduction in T_2^* (widely used in clinical practice).[2] In the setting of myocardial iron overload, T_1 also shortens, correlates strongly with T_2^*,[97,98] and has been validated histologically in animal models.[99] Native T_1-mapping may therefore become an alternative method for cardiac iron detection ($T_1 < 900$ ms at 1.5 T) and quantification with the potential advantages of fewer image artifacts, improved identification of mild iron loading, and superior reproducibility.[97] T_2 also correlates with T_2^* and extent of iron deposition,[99] and weaker (but significant) inverse associations have been described between T_2^* and ECV.[98]

Hypertrophic Cardiomyopathy

In a study of 130 HCM patients and 25 controls, T_1-mapping was employed to evaluate both regional and diffuse patterns of myocardial fibrosis. Postcontrast T_1 times were reduced in HCM (Figure 6), and while greater quantities of LGE were associated with reduced LV systolic function and less outflow tract obstruction, patients with lower postcontrast T_1 had more severe diastolic impairment and dyspnea.[59]

Native T_1 and ECV are also increased in HCM.[34,37,65] Native T_1 abnormalities have been reported in myocardial segments without LGE in HCM patients,[37,65] although ECV was similar to that of healthy controls in 1 study.[100] This may be explained by the concomitant presence of hypertrophic myocytes; thus, total ECV (ECV × myocardial mass) could be a better indicator of expansion in patients with HCM or amyloidosis.[92] Extracellular volume and, particularly, native T_1-mapping appear able to differentiate both HCM from hypertensive heart disease and sarcomere mutation carriers from normal controls, even in the absence of LV hypertrophy or LGE.[42,101] These data provide additional support that fibrotic remodeling is triggered early in the disease process.

The ongoing Hypertrophic Cardiomyopathy Registry (NCT01915615), an international multicenter study planning to enroll 2750 HCM patients, is expected to provide important insights into the potential clinical value of T_1-mapping in this disease.[102]

Congenital Heart Disease

T_1-mapping was performed in the systemic ventricle of 50 adults with various congenital abnormalities, demonstrating increased ECV, particularly in those with a systemic right ventricle

and/or cyanotic disease.[103] A recent publication also observed diffuse myocardial fibrosis in patients with repaired tetralogy of Fallot, and noted that biventricular ECV values were increased and positively correlated, likely secondary to an adverse interventricular interaction. Increased ECV was associated with both right ventricular volume overload and arrhythmia[104] and may play a role in prognostication in these patients.[105]

Valvular Heart Disease

As shown in Table 3, several validation studies have demonstrated increases in native myocardial T_1 and ECV in patients with aortic stenosis, with corresponding increases in interstitial fibrosis on histological samples. In young individuals with congenital aortic stenosis, ECV was higher than in normal participants and correlated with echocardiographic indexes of diastolic dysfunction.[106] Although in that study ECV was not associated with stenosis severity, reports in older adults with degenerative disease have demonstrated such correlations, as well as associations with impaired LV diastolic and systolic performance.[53,54,107]

Regarding regurgitant lesions, a cross-sectional study compared 35 patients with asymptomatic moderate or severe primary degenerative mitral regurgitation and no class I indication for surgery with age- and sex-matched controls. Extracellular volume was increased in patients and was associated with increased LV and left atrial volumes, as well as reduced systolic function and peak oxygen consumption.[108]

Prognosis

The potential predictive significance of mapping indices is being actively explored. Early studies suggest ECV may be at least as prognostically meaningful as LV ejection fraction and highlight the role of myocardial interstitium in driving patient "vulnerability".[63,109] A large single-center series[109] included 1172 consecutive patients without amyloidosis, HCM, or stress cardiomyopathy referred for CMR, and demonstrated an increased risk of death or hospitalization for heart failure over a median of 1.7 years (hazard ratio [HR] = 1.85 for every 5% increase in ECV; 95%CI, 1.50–2.2.7), adjusting for multiple confounders including age, LV ejection fraction, and MI size. The same group reported comparable prognostic significance in diabetics.[63] In another series of 473 consecutive patient referred for CMR and without HCM, amyloid, or Anderson-Fabry disease, ECV was a predictor of subsequent cardiovascular events although it did not remain significant after adjustment for clinical variables.[60] Extracellular volume calculated without direct hematocrit
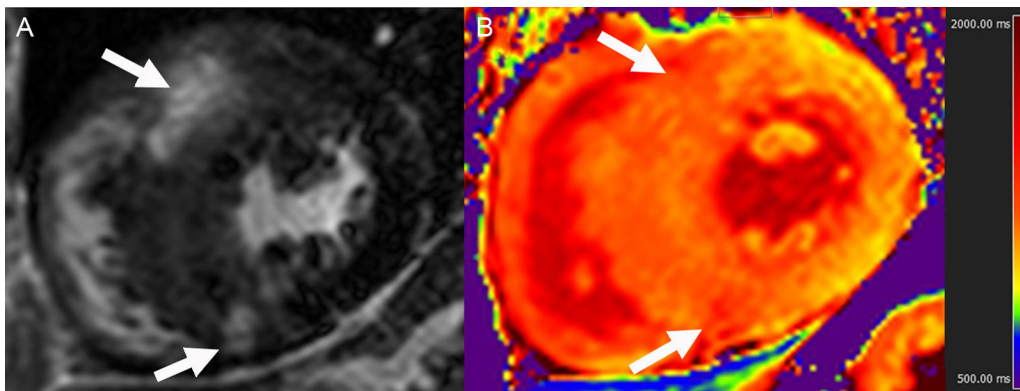

Figure 6. Late gadolinium enhancement short-axis view (A) and corresponding native T_1 map at 3 T (B) in a patient with hypertrophic cardiomyopathy. Note the increased T_1 in the septum compared with the lateral wall, particularly in the areas of late gadolinium enhancement (arrows).

measurement has also shown an ability to predict mortality (HR = 1.9 for every 5% increase in ECV; 95%CI, 1.55-2.31).[16]

The above-mentioned studies have studied the associations of T_1-mapping in unselected populations referred for CMR. More recently, a prospective, multicenter registry identified native T_1 as the strongest independent predictor of mortality and heart failure hospitalization in 637 patients with nonischemic DCM followed-up for a median of 22 months.[110] Another prospective study of 100 patients with ischemic and nonischemic DCM undergoing defibrillator implantation identified native T_1 as an independent predictor of appropriate antiarrhythmic therapy on follow-up.[111] In a prospective study of 100 subjects with heart failure with preserved ejection fraction, postcontrast T_1, left atrial area, and pulmonary vascular resistance were significantly associated with outcome (death or heart failure hospitalization).[57] In cardiac amyloidosis, visual determination of abnormal postcontrast myocardial T_1 and contrast kinetics on a look-locker sequence was the strongest predictor of mortality (adjusted HR = 5.5; 95%CI, 2.7-11.0; $P < .0001$) in 90 patients with suspected cardiac involvement.[112] In a recent series of 100 patients with systemic light-chain amyloidosis followed-up for a median of 23 months, both native T_1 (> 1044 ms at 1.5 T) and ECV ($> 45\%$) were markers of increased risk of death, and ECV remained significantly associated with mortality in multivariate models (adjusted HR = 4.4; 95%CI, 1.4-14.4; $P = .01$).[94]

Although demonstration of edema with standard T_2-weighted imaging has been linked to outcomes in acute coronary syndromes,[113] no study has yet explored the potential prognostic implications of T_2-mapping.

FUTURE DIRECTIONS

Myocardial mapping with CMR is rapidly evolving into a useful approach for the diagnosis and characterization of various cardiomyopathies, providing objective, quantitative measurements even without the need for contrast agents. Nonetheless, a number of challenges still remain that need to be met before widespread clinical implementation. As previously discussed, different approaches for the quantification of myocardial T_1 and T_2 times have specific strengths and limitations and provide slightly different values (Table 1 and Table 2). Therefore, myocardial mapping will need to be standardized in a fashion similar to LGE imaging. In the meantime, results cannot necessarily be extrapolated across sequences, vendors, or sites, and centers performing T_1- and T_2-mapping should develop their own set of normative, reference values.[6,15] Most sequences are sensitive to the presence of arrhythmia and there is also potential for errors from acquisition or analysis[6,24,48]; nonetheless, there is good interstudy and interscanner reproducibility, particularly for T_1-mapping[29,35,55,114] but also for T_2-mapping.[26,48] This indicates potential for use in clinical trials,[115] and the feasibility of testing the effect of therapies has already been shown in animal models.[116] It must be acknowledged, however, that myocardial mapping today is still not widely available, remains largely a research application, and in the United States it is not yet approved for clinical use.

Similar to LGE, abnormalities in myocardial relaxation times are nonspecific. While T_2 lengthening is largely reflective of inflammation, and the number of diseases leading to native T_1 shortening is limited, increases in native T_1 and ECV can be found in virtually any cardiac disorder (Table 4). Thus, myocardial maps today are of limited use as stand-alone techniques and need to be interpreted within the clinical context. In addition, the diagnostic ability of myocardial mapping has often been tested against healthy controls, whereas in clinical practice differential diagnosis is more

often needed in patients presenting with similar symptoms to those with the potential index disease. Finally, more and larger studies are needed to establish the incremental diagnostic and prognostic value of CMR mapping when accounting for other clinical variables, as well as the potential for guiding therapeutic interventions.

CONFLICTS OF INTEREST

None declared.

REFERENCES

1. Valbuena-Lopez S, Hinojar R, Puntmann VO. Cardiovascular Magnetic Resonance in Cardiology Practice: A Concise Guide to Image Acquisition and Clinical Interpretation. Rev Esp Cardiol. 2016;69:202–10.
2. Salerno M, Kramer CM. Advances in parametric mapping with CMR imaging. JACC Cardiovasc Imaging. 2013;6:806–22.
3. Plewes DB, Kucharczyk W. Physics of MRI: a primer. J Magn Reson Imaging. 2012;35:1038–54.
4. Baessler B, Schaarschmidt F, Stehning C, Schnackenburg B, Maintz D, Bunck AC. A systematic evaluation of three different cardiac T2-mapping sequences at 1.5 and 3T in healthy volunteers. Eur J Radiol. 2015;84:2161–70.
5. Mewton N, Liu CY, Croisille P, Bluemke D, Lima JA. Assessment of myocardial fibrosis with cardiovascular magnetic resonance. J Am Coll Cardiol. 2011;57: 891–903.
6. Moon JC, Messroghli DR, Kellman P, Piechnik SK, Robson MD, Ugander M, et al. Myocardial T1 mapping and extracellular volume quantification: a Society for Cardiovascular Magnetic Resonance (SCMR) and CMR Working Group of the European Society of Cardiology consensus statement. J Cardiovasc Magn Reson. 2013;15:92.
7. Taylor AJ, Salerno M, Dharmakumar R, Jerosch-Herold M. T1 Mapping: Basic Techniques and Clinical Applications. JACC Cardiovasc Imaging. 2016;9:67–81.
8. Iles L, Pfluger H, Phrommintikul A, Cherayath J, Aksit P, Gupta SN, et al. Evaluation of diffuse myocardial fibrosis in heart failure with cardiac magnetic resonance contrast-enhanced T1 mapping. J Am Coll Cardiol. 2008;52: 1574–80.
9. Messroghli DR, Plein S, Higgins DM, Walters K, Jones TR, Ridgway JP, et al. Human myocardium: single-breath-hold MR T1 mapping with high spatial resolution-reproducibility study. Radiology. 2006;238:1004–12.
10. Messroghli DR, Greiser A, Frohlich M, Dietz R, Schulz-Menger J. Optimization and validation of a fully-integrated pulse sequence for modified look-locker inversion-recovery (MOLLI) T1 mapping of the heart. J Magn Reson Imaging. 2007;26:1081–6.
11. Gai ND, Sandfort V, Liu S, Lima JA, Bluemke DA. Dose correction for postcontrast T1 mapping of the heart: the MESA study. Int J Cardiovasc Imaging. 2016;32:271–9.
12. Piechnik SK, Ferreira VM, Dall'Armellina E, Cochlin LE, Greiser A, Neubauer S, et al. Shortened Modified Look-Locker Inversion recovery (ShMOLLI) for clinical myocardial T1-mapping at 1.5 and 3 T within a 9 heartbeat breathhold. J Cardiovasc Magn Reson. 2010;12:69.
13. Arheden H, Saeed M, Higgins CB, Gao DW, Bremerich J, Wyttenbach R, et al. Measurement of the distribution volume of gadopentetate dimeglumine at echo-planar MR imaging to quantify myocardial infarction: comparison with 99mTc-DTPA autoradiography in rats. Radiology. 1999;211:698–708.
14. Nacif MS, Turkbey EB, Gai N, Nazarian S, Van der Geest RJ, Noureldin RA, et al. Myocardial T1 mapping with MRI: comparison of look-locker and MOLLI sequences. J Magn Reson Imaging. 2011;34:1367–73.
15. Schelbert EB, Messroghli DR. State of the Art: Clinical Applications of Cardiac T1 Mapping. Radiology. 2016;278:658–76.
16. Treibel TA, Fontana M, Maestrini V, Castelletti S, Rosmini S, Simpson J, et al. Automatic Measurement of the Myocardial Interstitium: Synthetic Extracellular Volume Quantification Without Hematocrit Sampling. JACC Cardiovasc Imaging. 2016;9:54–63.
17. Schelbert EB, Testa SM, Meier CG, Ceyrolles WJ, Levenson JE, Blair AJ, et al. Myocardial extravascular extracellular volume fraction measurement by gadolinium cardiovascular magnetic resonance in humans: slow infusion vs bolus. J Cardiovasc Magn Reson. 2011;13:16.
18. White SK, Sado DM, Fontana M, Banypersad SM, Maestrini V, Flett AS, et al. T1 mapping for myocardial extracellular volume measurement by CMR: bolus only vs primed infusion technique. JACC Cardiovasc Imaging. 2013;6:955–62.
19. Dabir D, Child N, Kalra A, Rogers T, Gebker R, Jabbour A, et al. Reference values for healthy human myocardium using a T1 mapping methodology: results from the International T1 Multicenter cardiovascular magnetic resonance study. J Cardiovasc Magn Reson. 2014;16:69.
20. Mongeon FP, Jerosch-Herold M, Coelho-Filho OR, Blankstein R, Falk RH, Kwong RY. Quantification of extracellular matrix expansion by CMR in infiltrative heart disease. JACC Cardiovasc Imaging. 2012;5:897–907.

21. Higgins CB, Herfkens R, Lipton MJ, Sievers R, Sheldon P, Kaufman L, et al. Nuclear magnetic resonance imaging of acute myocardial infarction in dogs: alterations in magnetic relaxation times. Am J Cardiol. 1983;52:184–8.

22. Flett AS, Hayward MP, Ashworth MT, Hansen MS, Taylor AM, Elliott PM, et al. Equilibrium contrast cardiovascular magnetic resonance for the measurement of diffuse myocardial fibrosis: preliminary validation in humans. Circulation. 2010;122:138–44.

23. Messroghli DR, Radjenovic A, Kozerke S, Higgins DM, Sivananthan MU, Ridgway JP. Modified Look-Locker inversion recovery (MOLLI) for high-resolution T1 mapping of the heart. Magn Reson Med. 2004;52:141–6.

24. Kellman P, Hansen MS. T1-mapping in the heart: accuracy and precision. J Cardiovasc Magn Reson. 2014;16:2.

25. Giri S, Chung YC, Merchant A, Mihai G, Rajagopalan S, Raman SV, et al. T2 quantification for improved detection of myocardial edema. J Cardiovasc Magn Reson. 2009;11:56.

26. Sprinkart AM, Luetkens JA, Traber F, Doerner J, Gieseke J, Schnackenburg B, et al. Gradient Spin Echo (GraSE) imaging for fast myocardial T2 mapping. J Cardiovasc Magn Reson. 2015;17:12.

27. Thavendiranathan P, Walls M, Giri S, Verhaert D, Rajagopalan S, Moore S, et al. Improved detection of myocardial involvement in acute inflammatory cardiomyopathies using T2 mapping. Circ Cardiovasc Imaging. 2012;5:102–10.

28. Von Knobelsdorff-Brenkenhoff F, Prothmann M, Dieringer MA, Wassmuth R, Greiser A, Schwenke C, et al. Myocardial T1 and T2 mapping at 3 T: reference values, influencing factors and implications. J Cardiovasc Magn Reson. 2013;15:53.

29. Rogers T, Dabir D, Mahmoud I, Voigt T, Schaeffter T, Nagel E, et al. Standardization of T1 measurements with MOLLI in differentiation between health and disease-the ConSept study. J Cardiovasc Magn Reson. 2013;15:78.

30. Reiter U, Reiter G, Dorr K, Greiser A, Maderthaner R, Fuchsjager M. Normal diastolic and systolic myocardial T1 values at 1.5-T MR imaging: correlations and blood normalization. Radiology. 2014;271:365–72.

31. Fontana M, White SK, Banypersad SM, Sado DM, Maestrini V, Flett AS, et al. Comparison of T1 mapping techniques for ECV quantification. Histological validation and reproducibility of ShMOLLI vs multibreath-hold T1 quantification equilibrium contrast CMR. J Cardiovasc Magn Reson. 2012;14:88.

32. Luetkens JA, Homsi R, Sprinkart AM, Doerner J, Dabir D, Kuetting DL, et al. Incremental value of quantitative CMR including parametric mapping for the diagnosis of acute myocarditis. Eur Heart J Cardiovasc Imaging. 2016;17:154–61.

33. Kellman P, Wilson JR, Xue H, Bandettini WP, Shanbhag SM, Druey KM, et al. Extracellular volume fraction mapping in the myocardium, part 2: initial clinical experience. J Cardiovasc Magn Reson. 2012;14:64.

34. Sado DM, Flett AS, Banypersad SM, White SK, Maestrini V, Quarta G, et al. Cardiovascular magnetic resonance measurement of myocardial extracellular volume in health and disease. Heart. 2012;98:1436–41.

35. Piechnik SK, Ferreira VM, Lewandowski AJ, Ntusi NA, Banerjee R, Holloway C, et al. Normal variation of magnetic resonance T1 relaxation times in the human population at 1.5 T using ShMOLLI. J Cardiovasc Magn Reson. 2013;15:13.

36. Liu CY, Liu YC, Wu C, Armstrong A, Volpe GJ, Van der Geest RJ, et al. Evaluation of age-related interstitial myocardial fibrosis with cardiac magnetic resonance contrast-enhanced T1 mapping: MESA (Multi-Ethnic Study of Atherosclerosis). J Am Coll Cardiol. 2013;62:1280–7.

37. Puntmann VO, Voigt T, Chen Z, Mayr M, Karim R, Rhode K, et al. Native T1 mapping in differentiation of normal myocardium from diffuse disease in hypertrophic and dilated cardiomyopathy. JACC Cardiovasc Imaging. 2013;6:475–84.

38. Neilan TG, Coelho-Filho OR, Shah RV, Abbasi SA, Heydari B, Watanabe E, et al. Myocardial extracellular volume fraction from T1 measurements in healthy volunteers and mice: relationship to aging and cardiac dimensions. JACC Cardiovasc Imaging. 2013;6:672–83.

39. Liu CY, Bluemke DA, Gerstenblith G, Zimmerman SL, Li J, Zhu H, et al. Reference values of myocardial structure, function, and tissue composition by cardiac magnetic resonance in healthy African-Americans at 3T and their relations to serologic and cardiovascular risk factors. Am J Cardiol. 2014;114:789–95.

40. Ugander M, Oki AJ, Hsu LY, Kellman P, Greiser A, Aletras AH, et al. Extracellular volume imaging by magnetic resonance imaging provides insights into overt and sub-clinical myocardial pathology. Eur Heart J. 2012;33:1268–78.

41. Miller CA, Naish JH, Bishop P, Coutts G, Clark D, Zhao S, et al. Comprehensive validation of cardiovascular magnetic resonance techniques for the assessment of myocardial extracellular volume. Circ Cardiovasc Imaging. 2013;6:373–83.

42. Hinojar R, Varma N, Child N, Goodman B, Jabbour A, Yu CY, et al. T1 Mapping in Discrimination of Hypertrophic Phenotypes: Hypertensive Heart Disease and Hypertrophic Cardiomyopathy: Findings From the International T1 Multicenter Cardiovascular Magnetic Resonance Study. Circ Cardiovasc Imaging. 2015. Available at: http://dx.doi.org/10.1161/CIRCIMAGING.115.003285

43. Aus dem Siepen F, Buss SJ, Messroghli D, Andre F, Lossnitzer D, Seitz S, et al. T1 mapping in dilated cardiomyopathy with cardiac magnetic resonance: quantification of diffuse myocardial fibrosis and comparison with endomyocardial biopsy. Eur Heart J Cardiovasc Imaging. 2015;16:210–6.

44. Langhans B, Nadjiri J, Jahnichen C, Kastrati A, Martinoff S, Hadamitzky M. Reproducibility of area at risk assessment in acute myocardial infarction by T1- and T2-mapping sequences in cardiac magnetic resonance imaging in comparison to Tc99m-sestamibi SPECT. Int J Cardiovasc Imaging. 2014;30:1357–63.

45. Ferreira VM, Piechnik SK, Dall'Armellina E, Karamitsos TD, Francis JM, Ntusi N, et al. T(1) mapping for the diagnosis of acute myocarditis using CMR: comparison to T2-weighted and late gadolinium enhanced imaging. JACC Cardiovasc Imaging. 2013;6:1048–58.

46. Radunski UK, Lund GK, Stehning C, Schnackenburg B, Bohnen S, Adam G, et al. CMR in patients with severe myocarditis: diagnostic value of quantitative tissue markers including extracellular volume imaging. JACC Cardiovasc Imaging. 2014;7:667–75.

47. Mordi I, Carrick D, Bezerra H, Tzemos N. T1 and T2 mapping for early diagnosis of dilated non-ischaemic cardiomyopathy in middle-aged patients and differentiation from normal physiological adaptation. Eur Heart J Cardiovasc Imaging. 2016;17:797–803.

48. Wassmuth R, Prothmann M, Utz W, Dieringer M, Von Knobelsdorff-Brenkenhoff F, Greiser A, et al. Variability and homogeneity of cardiovascular magnetic resonance myocardial T2-mapping in volunteers compared with patients with edema. J Cardiovasc Magn Reson. 2013;15:27.

49. Bonner F, Janzarik N, Jacoby C, Spieker M, Schnackenburg B, Range F, et al. Myocardial T2 mapping reveals age- and sex-related differences in volunteers. J Cardiovasc Magn Reson. 2015;17:9.

50. Verhaert D, Thavendiranathan P, Giri S, Mihai G, Rajagopalan S, Simonetti OP, et al. Direct T2 quantification of myocardial edema in acute ischemic injury. JACC Cardiovasc Imaging. 2011;4:269–78.

51. Bohnen S, Radunski UK, Lund GK, Kandolf R, Stehning C, Schnackenburg B, et al. Performance of T1 and T2 mapping cardiovascular magnetic resonance to detect active myocarditis in patients with recent-onset heart failure. Circ Cardiovasc Imaging. 2015. Available at: http://dx.doi.org/10.1161/CIRCIMAGING.114.003073

52. Usman AA, Taimen K, Wasielewski M, McDonald J, Shah S, Giri S, et al. Cardiac magnetic resonance T2 mapping in the monitoring and follow-up of acute cardiac transplant rejection: a pilot study. Circ Cardiovasc Imaging. 2012;5:782–90.

53. Bull S, White SK, Piechnik SK, Flett AS, Ferreira VM, Loudon M, et al. Human non-contrast T1 values and correlation with histology in diffuse fibrosis. Heart. 2013;99:932–7.

54. Lee SP, Lee W, Lee JM, Park EA, Kim HK, Kim YJ, et al. Assessment of diffuse myocardial fibrosis by using MR imaging in asymptomatic patients with aortic stenosis. Radiology. 2015;274:359–69.

55. De Meester de Ravenstein C, Bouzin C, Lazam S, Boulif J, Amzulescu M, Melchior J, et al. Histological Validation of measurement of diffuse interstitial myocardial fibrosis by myocardial extravascular volume fraction from Modified Look-Locker imaging (MOLLI) T1 mapping at 3 T. J Cardiovasc Magn Reson. 2015;17:48.

56. Sibley CT, Noureldin RA, Gai N, Nacif MS, Liu S, Turkbey EB, et al. T1 Mapping in cardiomyopathy at cardiac MR: comparison with endomyocardial biopsy. Radiology. 2012;265:724–32.

57. Mascherbauer J, Marzluf BA, Tufaro C, Pfaffenberger S, Graf A, Wexberg P, et al. Cardiac magnetic resonance postcontrast T1 time is associated with outcome in patients with heart failure and preserved ejection fraction. Circ Cardiovasc Imaging. 2013;6:1056–65.

58. Iles LM, Ellims AH, Llewellyn H, Hare JL, Kaye DM, McLean CA, et al. Histological validation of cardiac magnetic resonance analysis of regional and diffuse interstitial myocardial fibrosis. Eur Heart J Cardiovasc Imaging. 2015;16:14–22.

59. Ellims AH, Iles LM, Ling LH, Chong B, Macciocca I, Slavin GS, et al. A comprehensive evaluation of myocardial fibrosis in hypertrophic cardiomyopathy with cardiac magnetic resonance imaging: linking genotype with fibrotic phenotype. Eur Heart J Cardiovasc Imaging. 2014;15:1108–16.

60. Kammerlander AA, Marzluf BA, Zotter-Tufaro C, Aschauer S, Duca F, Bachmann A, et al. T1 Mapping by CMR Imaging: From Histological Validation to Clinical Implication. JACC Cardiovasc Imaging. 2016;9:14–23.

61. Fernandez-Jimenez R, Sanchez-Gonzalez J, Aguero J, Del Trigo M, Galan-Arriola C, Fuster V, et al. Fast T2 gradient-spin-echo (T2-GraSE) mapping for myocardial edema quantification: first in vivo validation in a porcine model of ischemia/reperfusion. J Cardiovasc Magn Reson. 2015;17:92.

62. Kuruvilla S, Janardhanan R, Antkowiak P, Keeley EC, Adenaw N, Brooks J, et al. Increased extracellular volume and altered mechanics are associated with LVH in hypertensive heart disease, not hypertension alone. JACC Cardiovasc Imaging. 2015;8:172–80.

63. Wong TC, Piehler KM, Kang IA, Kadakkal A, Kellman P, Schwartzman DS, et al. Myocardial extracellular volume fraction quantified by cardiovascular magnetic resonance is increased in diabetes and associated with mortality and incident heart failure admission. Eur Heart J. 2014;35:657–64.

64. Yi CJ, Wu CO, Tee M, Liu CY, Volpe GJ, Prince MR, et al. The association between cardiovascular risk and cardiovascular magnetic resonance measures of fibrosis: the Multi-Ethnic Study of Atherosclerosis (MESA). J Cardiovasc Magn Reson. 2015;17:15.

65. Dass S, Suttie JJ, Piechnik SK, Ferreira VM, Holloway CJ, Banerjee R, et al. Myocardial tissue characterization using magnetic resonance noncontrast t1 mapping in hypertrophic and dilated cardiomyopathy. Circ Cardiovasc Imaging. 2012;5:726–33.

66. Donekal S, Venkatesh BA, Liu YC, Liu CY, Yoneyama K, Wu CO, et al. Interstitial fibrosis, left ventricular remodeling, and myocardial mechanical behavior in a population-based multiethnic cohort: the Multi-Ethnic Study of Atherosclerosis (MESA) study. Circ Cardiovasc Imaging. 2014;7:292–302.

67. Garcia-Alvarez A, Garcia-Lunar I, Pereda D, Fernandez-Jimenez R, Sanchez-Gonzalez J, Mirelis JG, et al. Association of myocardial T1-mapping CMR with

hemodynamics and RV performance in pulmonary hypertension. JACC Cardiovasc Imaging. 2015;8:76–82.

68. Mehta BB, Auger DA, Gonzalez JA, Workman V, Chen X, Chow K, et al. Detection of elevated right ventricular extracellular volume in pulmonary hypertension using Accelerated and Navigator-Gated Look-Locker Imaging for Cardiac T1 Estimation (ANGIE) cardiovascular magnetic resonance. J Cardiovasc Magn Reson. 2015;17:110.

69. Pozo E, Sanz J. Imaging Techniques in the Evaluation of Postinfarction Function and Scar. Rev Esp Cardiol. 2014;67:754–64.

70. McAlindon EJ, Pufulete M, Harris JM, Lawton CB, Moon JC, Manghat N, et al. Measurement of myocardium at risk with cardiovascular MR: comparison of techniques for edema imaging. Radiology. 2015;275:61–70.

71. Ferreira VM, Piechnik SK, Dall'Armellina E, Karamitsos TD, Francis JM, Choudhury RP, et al. Non-contrast T1-mapping detects acute myocardial edema with high diagnostic accuracy: a comparison to T2-weighted cardiovascular magnetic resonance. J Cardiovasc Magn Reson. 2012;14:42.

72. Ugander M, Bagi PS, Oki AJ, Chen B, Hsu LY, Aletras AH, et al. Myocardial edema as detected by pre-contrast T1 and T2 CMR delineates area at risk associated with acute myocardial infarction. JACC Cardiovasc Imaging. 2012;5:596–603.

73. Fernandez-Jimenez R, Sanchez-Gonzalez J, Aguero J, Garcia-Prieto J, Lopez-Martin GJ, Garcia-Ruiz JM, et al. Myocardial edema after ischemia/reperfusion is not stable and follows a bimodal pattern: imaging and histological tissue characterization. J Am Coll Cardiol. 2015;65:315–23.

74. Messroghli DR, Walters K, Plein S, Sparrow P, Friedrich MG, Ridgway JP, et al. Myocardial T1 mapping: application to patients with acute and chronic myocardial infarction. Magn Reson Med. 2007;58:34–40.

75. Hammer-Hansen S, Bandettini WP, Hsu LY, Leung SW, Shanbhag S, Mancini C, et al. Mechanisms for overestimating acute myocardial infarct size with gadolinium-enhanced cardiovascular magnetic resonance imaging in humans: a quantitative and kinetic study. Eur Heart J Cardiovasc Imaging. 2016;17:76–84.

76. Kali A, Choi EY, Sharif B, Kim YJ, Bi X, Spottiswoode B, et al. Native T1 Mapping by 3-T CMR Imaging for Characterization of Chronic Myocardial Infarctions. JACC Cardiovasc Imaging. 2015;8:1019–30.

77. Carrick D, Haig C, Rauhalammi S, Ahmed N, Mordi I, McEntegart M, et al. Prognostic significance of infarct core pathology revealed by quantitative non-contrast in comparison with contrast cardiac magnetic resonance imaging in reperfused ST-elevation myocardial infarction survivors. Eur Heart J. 2016;37:1044–59.

78. Liu A, Wijesurendra RS, Francis JM, Robson MD, Neubauer S, Piechnik SK, et al. Adenosine Stress and Rest T1 Mapping Can Differentiate Between Ischemic, Infarcted, Remote, and Normal Myocardium Without the Need for Gadolinium Contrast Agents. JACC Cardiovasc Imaging. 2016;9:27–36.

79. Friedrich MG, Sechtem U, Schulz-Menger J, Holmvang G, Alakija P, Cooper LT, et al. Cardiovascular magnetic resonance in myocarditis: A JACC White Paper. J Am Coll Cardiol. 2009;53:1475–87.

80. Ferreira VM, Piechnik SK, Dall'Armellina E, Karamitsos TD, Francis JM, Ntusi N, et al. Native T1-mapping detects the location, extent and patterns of acute myocarditis without the need for gadolinium contrast agents. J Cardiovasc Magn Reson. 2014;16:36.

81. Luetkens JA, Doerner J, Thomas DK, Dabir D, Gieseke J, Sprinkart AM, et al. Acute myocarditis: multiparametric cardiac MR imaging. Radiology. 2014;273:383–92.

82. Hinojar R, Foote L, Arroyo Ucar E, Jackson T, Jabbour A, Yu CY, et al. Native T1 in discrimination of acute and convalescent stages in patients with clinical diagnosis of myocarditis: a proposed diagnostic algorithm using CMR. JACC Cardiovasc Imaging. 2015;8:37–46.

83. Crouser ED, Ono C, Tran T, He X, Raman SV. Improved detection of cardiac sarcoidosis using magnetic resonance with myocardial T2 mapping. Am J Respir Crit Care Med. 2014;189:109–12.

84. Marie PY, Angioi M, Carteaux JP, Escanye JM, Mattei S, Tzvetanov K, et al. Detection and prediction of acute heart transplant rejection with the myocardial T2 determination provided by a black-blood magnetic resonance imaging sequence. J Am Coll Cardiol. 2001;37:825–31.

85. Zhang Y, Corona-Villalobos CP, Kiani AN, Eng J, Kamel IR, Zimmerman SL, et al. Myocardial T2 mapping by cardiovascular magnetic resonance reveals subclinical myocardial inflammation in patients with systemic lupus erythematosus. Int J Cardiovasc Imaging. 2015;31:389–97.

86. Ntusi NA, Piechnik SK, Francis JM, Ferreira VM, Matthews PM, Robson MD, et al. Diffuse Myocardial Fibrosis and Inflammation in Rheumatoid Arthritis: Insights From CMR T1 Mapping. JACC Cardiovasc Imaging. 2015;8:526–36.

87. Ntusi NA, Piechnik SK, Francis JM, Ferreira VM, Rai AB, Matthews PM, et al. Subclinical myocardial inflammation and diffuse fibrosis are common in systemic sclerosis-a clinical study using myocardial T1-mapping and extracellular volume quantification. J Cardiovasc Magn Reson. 2014;16:21.

88. Puntmann VO, D'Cruz D, Smith Z, Pastor A, Choong P, Voigt T, et al. Native myocardial T1 mapping by cardiovascular magnetic resonance imaging in subclinical cardiomyopathy in patients with systemic lupus erythematosus. Circ Cardiovasc Imaging. 2013;6:295–301.

89. Garcia-Pavia P, Tome-Esteban MT, Rapezzi C. Amyloidosis. Also a heart disease. Rev Esp Cardiol. 2011;64:797–808.

90. Karamitsos TD, Piechnik SK, Banypersad SM, Fontana M, Ntusi NB, Ferreira VM, et al. Noncontrast T1 mapping for the diagnosis of cardiac amyloidosis. JACC Cardiovasc Imaging. 2013;6:488–97.

91. Fontana M, Banypersad SM, Treibel TA, Maestrini V, Sado DM, White SK, et al. Native T1 mapping in transthyretin amyloidosis. JACC Cardiovasc Imaging. 2014;7:157–65.

92. Fontana M, Banypersad SM, Treibel TA, Abdel-Gadir A, Maestrini V, Lane T, et al. Differential Myocyte Responses in Patients with Cardiac Transthyretin Amyloidosis and Light-Chain Amyloidosis: A Cardiac MR Imaging Study. Radiology. 2015;277:388–97.

93. Banypersad SM, Sado DM, Flett AS, Gibbs SD, Pinney JH, Maestrini V, et al. Quantification of myocardial extracellular volume fraction in systemic AL amyloidosis: an equilibrium contrast cardiovascular magnetic resonance study. Circ Cardiovasc Imaging. 2013;6:34–9.

94. Banypersad SM, Fontana M, Maestrini V, Sado DM, Captur G, Petrie A, et al. T1 mapping and survival in systemic light-chain amyloidosis. Eur Heart J. 2015;36:244–51.

95. Tham EB, Haykowsky MJ, Chow K, Spavor M, Kaneko S, Khoo NS, et al. Diffuse myocardial fibrosis by T1-mapping in children with subclinical anthracycline cardiotoxicity: relationship to exercise capacity, cumulative dose and remodeling. J Cardiovasc Magn Reson. 2013;15:48.

96. Sado DM, White SK, Piechnik SK, Banypersad SM, Treibel T, Captur G, et al. Identification and assessment of Anderson-Fabry disease by cardiovascular magnetic resonance noncontrast myocardial T1 mapping. Circ Cardiovasc Imaging. 2013;6:392–8.

97. Sado DM, Maestrini V, Piechnik SK, Banypersad SM, White SK, Flett AS, et al. Noncontrast myocardial T1 mapping using cardiovascular magnetic resonance for iron overload. J Magn Reson Imaging. 2015;41:1505–11.

98. Hanneman K, Nguyen ET, Thavendiranathan P, Ward R, Greiser A, Jolly MP, et al. Quantification of Myocardial Extracellular Volume Fraction with Cardiac MR Imaging in Thalassemia Major. Radiology. 2016;279:720–30.

99. Wood JC, Otto-Duessel M, Aguilar M, Nick H, Nelson MD, Coates TD, et al. Cardiac iron determines cardiac T2*, T2, and T1 in the gerbil model of iron cardiomyopathy. Circulation. 2005;112:535–43.

100. Brouwer WP, Baars EN, Germans T, De Boer K, Beek AM, Van der Velden J, et al. In-vivo T1 cardiovascular magnetic resonance study of diffuse myocardial fibrosis in hypertrophic cardiomyopathy. J Cardiovasc Magn Reson. 2014;16:28.

101. Ho CY, Abbasi SA, Neilan TG, Shah RV, Chen Y, Heydari B, et al. T1 measurements identify extracellular volume expansion in hypertrophic cardiomyopathy sarcomere mutation carriers with and without left ventricular hypertrophy. Circ Cardiovasc Imaging. 2013;6:415–22.

102. Kramer CM, Appelbaum E, Desai MY, Desvigne-Nickens P, DiMarco JP, Friedrich MG, et al. Hypertrophic Cardiomyopathy Registry: The rationale and design of an international, observational study of hypertrophic cardiomyopathy. Am Heart J. 2015;170:223–30.

103. Broberg CS, Chugh SS, Conklin C, Sahn DJ, Jerosch-Herold M. Quantification of diffuse myocardial fibrosis and its association with myocardial dysfunction in congenital heart disease. Circ Cardiovasc Imaging. 2010;3:727–34.

104. Chen CA, Dusenbery SM, Valente AM, Powell AJ, Geva T. Myocardial ECV Fraction Assessed by CMR Is Associated With Type of Hemodynamic Load and Arrhythmia in Repaired Tetralogy of Fallot. JACC Cardiovasc Imaging. 2016;9:1–10.

105. Broberg CS, Huang J, Hogberg I, McLarry J, Woods P, Burchill LJ, et al. Diffuse LV Myocardial Fibrosis and its Clinical Associations in Adults With Repaired Tetralogy of Fallot. JACC Cardiovasc Imaging. 2016;9:86–7.

106. Dusenbery SM, Jerosch-Herold M, Rickers C, Colan SD, Geva T, Newburger JW, et al. Myocardial extracellular remodeling is associated with ventricular diastolic dysfunction in children and young adults with congenital aortic stenosis. J Am Coll Cardiol. 2014;63:1778–85.

107. Chin CW, Semple S, Malley T, White AC, Mirsadraee S, Weale PJ, et al. Optimization and comparison of myocardial T1 techniques at 3T in patients with aortic stenosis. Eur Heart J Cardiovasc Imaging. 2014;15:556–65.

108. Edwards NC, Moody WE, Yuan M, Weale P, Neal D, Townend JN, et al. Quantification of left ventricular interstitial fibrosis in asymptomatic chronic primary degenerative mitral regurgitation. Circ Cardiovasc Imaging. 2014;7:946–53.

109. Schelbert EB, Piehler KM, Zareba KM, Moon JC, Ugander M, Messroghli DR, et al. Myocardial Fibrosis Quantified by Extracellular Volume Is Associated With Subsequent Hospitalization for Heart Failure, Death, or Both Across the Spectrum of Ejection Fraction and Heart Failure Stage. J Am Heart Assoc. 2015;4.

110. Puntmann VO, Carr-White G, Jabbour A, Yu CY, Gebker R, Kelle S, et al. T1-Mapping and Outcome in Nonischemic Cardiomyopathy: All-Cause Mortality and Heart Failure. JACC Cardiovasc Imaging. 2016;9:40–50.

111. Chen Z, Sohal M, Voigt T, Sammut E, Tobon-Gomez C, Child N, et al. Myocardial tissue characterization by cardiac magnetic resonance imaging using T1 mapping predicts ventricular arrhythmia in ischemic and non-ischemic cardiomyopathy patients with implantable cardioverter-defibrillators. Heart Rhythm. 2015;12:792–801.

112. White JA, Kim HW, Shah D, Fine N, Kim KY, Wendell DC, et al. CMR imaging with rapid visual T1 assessment predicts mortality in patients suspected of cardiac amyloidosis. JACC Cardiovasc Imaging. 2014;7:143–56.

113. Eitel I, Desch S, Fuernau G, Hildebrand L, Gutberlet M, Schuler G, et al. Prognostic significance and determinants of myocardial salvage assessed by cardiovascular magnetic resonance in acute reperfused myocardial infarction. J Am Coll Cardiol. 2010;55:2470–9.

114. Raman FS, Kawel-Boehm N, Gai N, Freed M, Han J, Liu CY, et al. Modified look-locker inversion recovery T1 mapping indices: assessment of accuracy and

reproducibility between magnetic resonance scanners. J Cardiovasc Magn Reson. 2013;15:64.

115. Liu S, Han J, Nacif MS, Jones J, Kawel N, Kellman P, et al. Diffuse myocardial fibrosis evaluation using cardiac magnetic resonance T1 mapping: sample size considerations for clinical trials. J Cardiovasc Magn Reson. 2012;14:90.

116. Stuckey DJ, McSweeney SJ, Thin MZ, Habib J, Price AN, Fiedler LR, et al. T(1) mapping detects pharmacological retardation of diffuse cardiac fibrosis in mouse pressure-overload hypertrophy. Circ Cardiovasc Imaging. 2014;7: 240–9.